

Soil Microbial Functional Succession Over One Year of Human Decomposition

Allison R. Mason¹, Lois S. Taylor², Naomi Gilbert¹,
Steven W. Wilhelm¹, Jennifer M. DeBruyn^{1,2*}

¹Department of Microbiology, University of Tennessee-Knoxville, 1311
Cumberland Avenue, Knoxville, 37996.

²Department of Biosystems Engineering and Soil Science, University of
Tennessee-Knoxville, 2506 E.J. Chapman Drive, Knoxville, 37996.

*Corresponding author(s). E-mail(s): jdeburyn@utk.edu;

Abstract

Background The succession of microbial communities during vertebrate decomposition has been observed in various settings, documenting changes in taxa as decomposition progresses. These studies have predominantly employed phylogenetic makers (*i.e.*, rRNA genes), describing community composition and structure, but ultimately do not inform about which members are active or metabolic pathways they might be expressing. This has left a foundational knowledge gap regarding the function roles microorganisms play in vertebrate decomposition, which ultimately impact ecosystem functioning. Here we present the first study investigating gene expression in soil impacted by human decomposition. Total RNA was extracted and metatranscriptomes obtained from soil samples collected over the course of one year from below three decomposing human bodies.

Results Microbial gene expression profiles shifted in response to decomposition: decomposition impacted soils were most different from controls (*i.e.* nearby soils unimpacted by decomposition) at day 86, and profiles remained altered even after

one year. Shifts in gene expression were partially explained by environmental and soil physiochemical variables, including internal body accumulated degree hours ($p = 0.001$), as well as soil temperature ($p = 0.045$), pH ($p = 0.042$) and electrical conductivity ($p = 0.037$). Differential expression analysis revealed that microbes in decomposition soils increased expression of stress response genes (mean fold change 3.48), particularly heat shock proteins ($p < 0.001$), whose expression increased between days 0 and 58 and remained elevated through day 376. Further, we identified genes whose expression was altered at certain timepoints. This included increased expression of nitrogen cycling genes HAO (85x), norB (83x), and nosZ (19x) at day 86 when dissolved oxygen was reduced to approximately 85%, suggesting that microbial communities may be converting hydroxylamine to nitric oxide during reduced oxygen conditions.

Conclusions Our results show that human decomposition alters soil microbial gene expression profiles providing evidence of altered microbial metabolisms (*e.g.*, taurine metabolism, nitrogen cycling, and lipid metabolism) and reveal the potential of vertebrate decomposition to have both ephemeral and lasting effects on ecosystem processing in response to mortality events.

Keywords: Human Decomposition, Microbial Succession, Metatranscriptomics, Soil Microbial Ecology

Introduction

Soil microbial communities are important drivers of ecosystem processes in terrestrial environments. Many soil microbes are decomposers that are involved in degradation of complex organic matter and drive nutrient cycling in terrestrial ecosystems. Environmental disturbances can impact the presence and/or activity of soil microorganisms that are involved in these cycles, ultimately affecting nutrient availability and the release of greenhouse gas emissions, such as CO₂ and N₂O [1, 2]. Vertebrate death, and subsequent carcass deposition in terrestrial ecosystems, is one disturbance that impact soil biogeochemical cycling and microbial community structure. Specifically altered elemental concentrations [3] and carbon (C) and nitrogen (N) transformations [4–10] have been observed in response to the release of concentrated decomposition products into the surrounding soil.

While C and N transformations have been documented during decomposition, the functional response of microbes and their roles in nutrient cycles remain unclear. Previous work from our lab [11, 12] and others [13–16] have conducted surveys of decomposition-impacted soil microbial communities through amplicon sequencing of marker genes(*i.e.*, 16S rRNA, 18S rRNA, ITS). This has allowed us to investigate how microbial biodiversity and composition change in response to vertebrate decomposition, revealing patterns such as increases in the anaerobic taxa *Firmicutes* and *Bacteroidetes*. However, few studies have investigated soil biogeochemistry and microbial communities within the same study, which can further help to describe microbial ecology in human and animal decomposition systems. Taylor et al. (2024) [17] suggested that observed fungal community shifts were linked to soil dissolved oxygen, highlighting interactions between soil microbes and the surrounding environment. Additionally, Metcalf et al. (2016) [14] started to connect microbial changes to physiochemical data (*e.g.*, nitrate, pH) during controlled mouse decomposition experiments. While insightful for making potential connections between taxa and physiochemistry, these analyses cannot inform which taxa are active members of the community responsible for chemical transformations, which functional pathways/genes are expressed, and how these pathways are altered in response to decomposition.

Methods such as RNA sequencing (*i.e.*, metatranscriptomics) and metabolomics can be used to investigate microbial community functional succession in response to decomposition by measuring gene expression and metabolites, respectively. Where DNA-based methods are limited to explaining structural succession, analysis of microbial community gene expression (*i.e.*, mRNA) helps to determine which functional pathways are altered in response to decomposition. This can inform how ecological functions, including C and N cycling, are impacted by decomposition events in terrestrial ecosystems. To date, only two studies have applied metatranscriptomic approaches to assess mRNA in vertebrate decomposition samples [18, 19]: Burcham et

al. (2019) [18] examined gene expression of internal organ microbial communities during mouse decomposition, while Ashe et al. (2021) [19] examined gene expression of oral microbial communities during human decomposition. Both studies suggest that the host microbial community functionality is altered during decomposition, including differential expression of amino acid and carbohydrate metabolism in the heart [18] and shifts in gene transcripts across different taxa [19]. We expect that soil microbial community gene expression profiles are also altered; however, this has never been examined. The decomposition-impacted soil metabolome was assessed by DeBruyn et al. (2021) [20], showing changes in soil metabolites over time, however it is unclear which microbes are responsible for these shifts. Additionally, DeBruyn et al. (2021) [20] showed the soil metabolome was still altered compared to starting conditions at the end of the 21-week study, suggesting long-term impacts of decomposition on soil microbial functioning.

The purpose of this study was to investigate soil microbial gene expression during a one-year period of human decomposition and address the following questions: (1) which genes are differentially expressed in soils impacted by human decomposition? (2) how does gene expression change over time in decomposition-impacted soils? (3) do microbial gene expression profiles return to pre-decomposition conditions after one year? The human body is comprised of carbon-rich organic molecules, many of which are broken down during decomposition. We hypothesized that gene expression would change over time as resources are used and transformed and soil chemical and physical conditions change as a result of tissue degradation [8, 9, 20]. For example, we expected to observe changes in the expression of genes encoding enzymes involved in nitrogen cycling, as increased nitrogen transformations have been previously described in decomposition soils [8]. Of the main macromolecules in the body (carbohydrates, proteins, lipids, and nucleic acids), we were particularly interested in lipid metabolism, as we expect lipids from the body to enter the soil during decomposition and previous

studies showed altered lipase activity in decomposition soils [21]. Finally, multiple studies have shown that soil chemistry [5, 8] and microbial community composition [11, 13] (via 16S rRNA gene amplicon sequencing) are still impacted after one year, therefore we did not expect soil expression profiles to return to pre-decomposition conditions.

To answer these questions, metatranscriptomics of soil samples collected at six key timepoints over one year of human decomposition were used to determine the active populations and expression of genes and pathways relevant to the enhanced biogeochemical cycling observed in decomposition hotspots. We compared gene expression between decomposition timepoints and control soils that were unexposed to decomposition products to identify functions or functional pathways of interest. This assessment of function profiles within decomposition-impacted soils provided insight into the microbial response to vertebrate decomposition in terrestrial settings and biogeochemical cycling within these hotspots.

Results

Soil Physiochemistry

As reported in the original study, soil chemistry was altered in response to human decomposition, with multiple parameters still impacted after one-year [17]. Generally, soil pH decreased and remained low in decomposition soils of all but one individual. Soil electrical conductivity (EC) increased in response to decomposition, remaining elevated through approximately day 58 before gradually decreasing throughout the remainder of the study (Supplementary Material 1). Respiration (evolved CO₂) increased by an order of magnitude beginning at day 12, which corresponded to a reduction in soil dissolved oxygen (DO) to 29% - 48.9%. Ammonium concentrations increased 78 fold, reaching maximum concentrations between days 12 and 58.

231 This was followed by decreased ammonium and increased nitrate concentrations at
232 day 86, with nitrate concentrations reaching a maximum at day 168 (Supplementary
233 Material [1](#)).
234
235

236

237 Sequencing

238

239 Illumina sequencing of the 24 libraries yielded a total of 5,073,476,730 reads, or
240 2,536,738,365 paired reads, with a mean of 105,697,432 paired reads per sample.
241 Removal of adapters and low-quality reads removed 4.7% of all reads, leaving
242 4,834,123,062 total reads. Filtering of ribosomal RNA further removed 7.3% of reads,
243 leaving 4,479,804,360 reads for assembly. After co-assembly, a total of 6,257,674 pro-
244 teins were identified by Prodigal. From this, 1,048,573 proteins were annotated by
245 eggNOG-mapper (16.7%). Most of the annotated proteins were taxonomically anno-
246 tated as bacteria (91.3%), followed by eukaryotes (7.6 %), and archaea (0.81 %). Of
247 the 7.6% of eukaryotic proteins, 64.4% (4.9% of all proteins) were annotated as fungi.
248 For this study, genes of interest included all bacterial, archaeal, and fungal proteins,
249 therefore all non-fungal eukaryotic proteins (32,004) were removed prior to down-
250 stream analysis. The reference file of genes was then used to determine gene transcript
251 counts in all samples using CLC genomic workbench. The percent of reads mapped
252 to genes of interest ranged from 21% to 38%, with an average of 31% reads mapped.
253 Gene counts were then combined in a single file and used for downstream analyses in
254 R.
255
256

257

258 Microbial gene expression in response to human decomposition

259

260 Gene expression profiles in decomposition-impacted soils shifted away from controls
261 and day zero samples as decomposition progressed (Fig [1A](#)). Expression was most
262 different from controls on study days 58, 86, 168 (Supplementary Material [2](#)), before
263
264
265
266

267

268

269

270

271

272

273

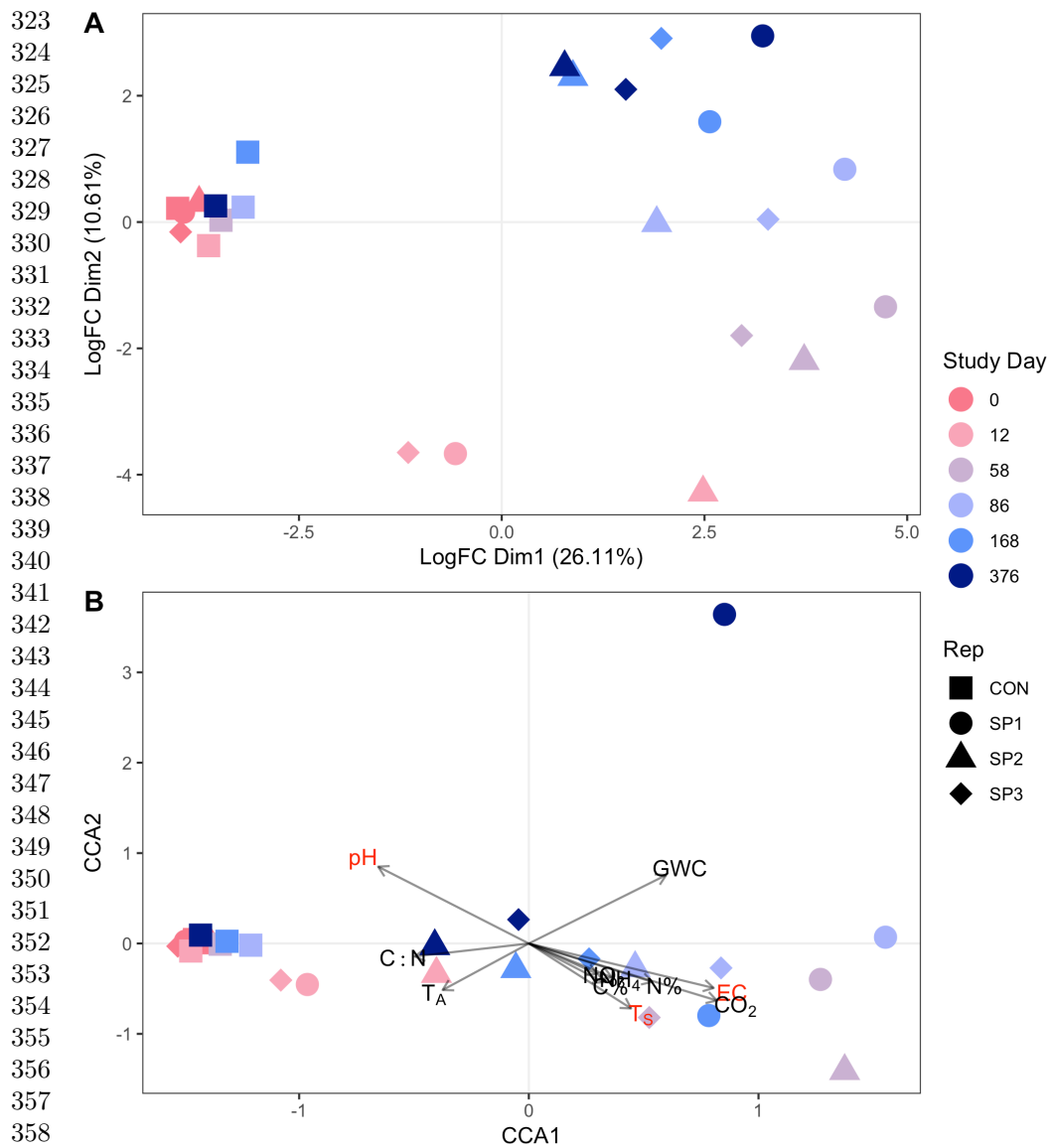
274

275

276

shifting back toward control conditions on study day 376. After one year of decomposition, soil gene expression profiles had not returned to pre-decomposition conditions, as evidenced by their clustering away from controls and day zero samples in the MDS plot (Fig 1A).

Figure 1: Microbial gene expression profiles are altered during human decomposition. Multidimensional scaling (MDS) shows gene expression within soils changed as decomposition progressed (A). Additionally, canonical correspondence analysis (CCA) shows that environmental variables explained 64.3% of the variation in gene expression profiles (B). Variables **bolded in red** significantly ($p < 0.05$) explained some of the variation in gene expression profiles as assessed by Permutational Analysis of Variance (PERMANOVA). In both panels, soils from controls (CON) and the three donors (SP1, SP2, SP3) are denoted by symbol shape, while color represents study day. In B, soil physiochemical variable loadings are represented by arrows: Gravimetric water content (GWC), electrical conductivity (EC), pH (pH), respiration (evolved CO_2 $\mu\text{mol gdw}^{-1}$), ammonium (NH_4), and nitrate (NO_3) concentrations (mg gdw^{-1}), percent carbon (%C), percent nitrogen (%N), carbon:nitrogen ratio (C:N), ambient temperature (T_A), and soil temperature (T_S).

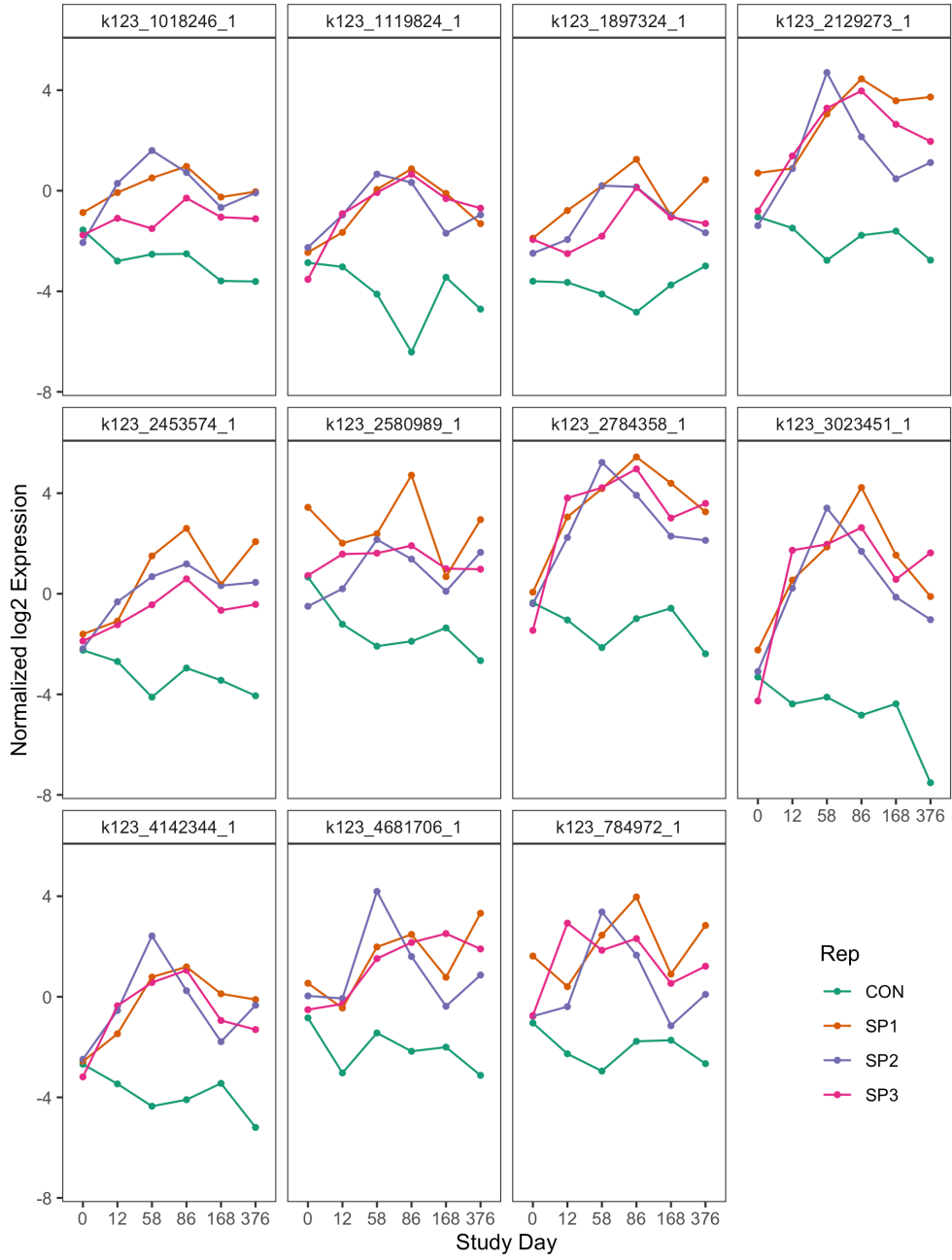


Some correlations were observed between gene expression shifts and soil physiochemical data at decomposition timepoints. Canonical correspondence analysis (CCA) was used to constrain gene expression data with soil physiochemical data (Fig 1B). CCA1 and CCA2 explained 36.2% and 20.9% of the variance in gene expression, respectively.

Transcript profiles at day 12 were associated with an increase in soil C:N. Gene expression profiles at days 58 to 86 were correlated with increased soil temperature, EC, and evolved CO₂, while study day 168 was associated with elevated levels of soil NO₃. Further, Permutational Analysis of Variance (PERMANOVA) revealed that internal ADH, soil temperature, pH, and EC significantly explained some of the variation in gene expression profiles ($p < 0.05$). No other variables were significant at $\alpha = 0.05$ (Supplementary Material 3).

Overall, decomposition changed soil gene expression profiles over the one-year study relative to control soils. Differential expression analysis between decomposition soils and control identified 7,047 down-regulated and 38,425 up-regulated genes. Gene transcripts that were associated with control soils were from a wide variety of clusters of orthologous genes (COG) functional categories. Specifically, the top 20 genes whose expression was higher in control soils belonged to ten unique COG categories, including signal transduction mechanisms, transcription, and those of unknown function. In contrast, the top 20 genes whose expression was higher in decomposition soils only fell into four COG categories (Supplementary Material 4 A): 1) post-translational modification, protein turnover, and chaperones; 2) energy production and conversion; 3) cell motility; and 4) carbohydrate transport and metabolism. The most common COG category represented in decomposition soils were post-translational modification, protein turnover, and chaperones. Within this category, several heat shock stress response genes were identified, including SSA2, HSP82, and clpB (Supplementary Material 5). Further investigation into these genes shows their expression increased in response to decomposition, typically reaching maximum transcript levels around study days 58 and 86 (Fig 2). This corresponded to elevated soil temperature below decomposing bodies between study days 12-80, with soil temperatures up to approximately 43°C [17], and maximum soil electrical conductivity measurements between days 12 and 58 (Supplementary Material 1).

Figure 2: Normalized log2 expression of heat shock proteins identified by differential expression analysis comparing decomposition and control soils. Symbol color denotes if the sample is a control (CON, green), or one of three individuals: SP1 (orange), SP2 (purple), or SP3 (pink).



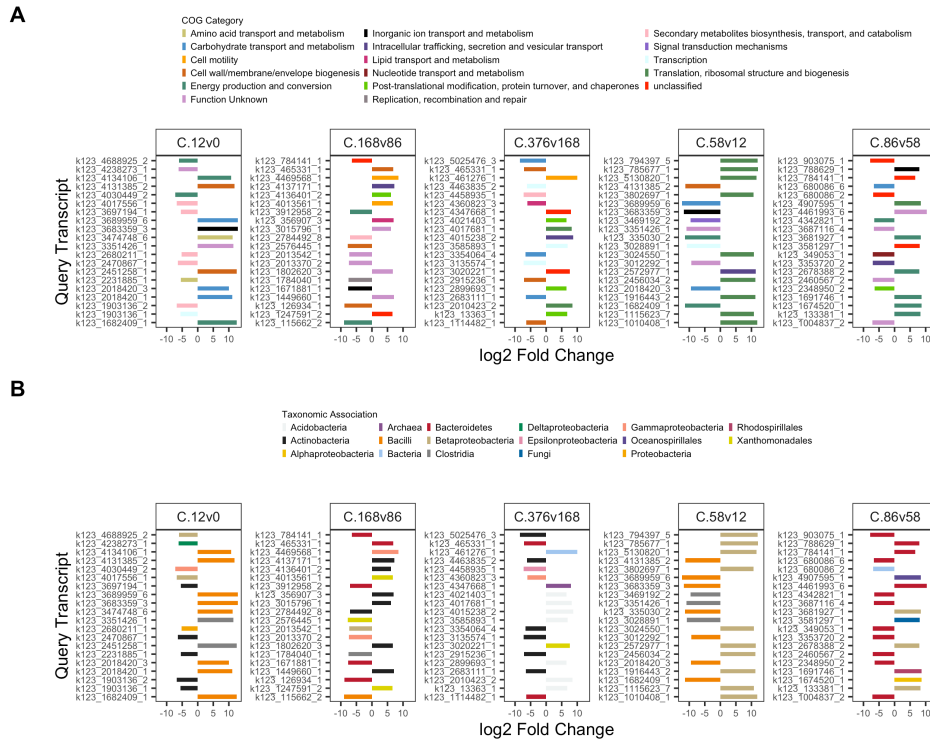
Taxonomy associated with top differentially expressed gene transcripts also differed between control and decomposition soils. The top 30 significantly differentially expressed gene transcripts in decomposition soils were associated with Fungi, *Actinobacteria*, and *Xanthomonadales*, while gene transcripts in controls were associated with *Acidobacteria*, *Cyanobacteria*, *Proteobacteria* (α , δ , γ), and Planctomycetes (Supplementary Material 4 B). The greatest number of differentially expressed genes relative to control samples was observed at day 86, where we saw 145,460 and 124,883 up- and down-regulated genes, respectively.

Fate of decomposition products as evidenced in gene expression profiles over time

Differential expression analysis between respective sequential study days further revealed which genes were altered between decomposition timepoints. The top ten significantly up- and down-regulated genes, determined by lowest p-values from differential expression analysis, are reported in Supplementary Material 6 and Fig 3.

Figure 3: Top twenty up- and down-regulated genes in decomposition soils comparing sequential study days (0, 12, 58, 86, 168, 376) colored by COG functional category (A) and taxonomic annotation (B). Positive values denote increased expression compared to the preceding timepoint, while negative values denote a decrease.

507
508
509
510
511
512
513
514
515
516
517
518
519
520
521
522
523
524
525
526
527
528
529
530
531
532
533
534
535
536
537
538
539
540
541
542
543
544
545
546
547
548
549
550
551
552



Expression of genes annotated with the COG categories cell wall/membrane/envelope biogenesis, inorganic ion transport and metabolism, and carbohydrate transport and metabolism increased from day 0 to 12. In contrast, expression of secondary metabolite biosynthesis, transport, and catabolism genes decreased during this period (Fig 3A). Transcripts from *Bacilli* and *Clostridia* increased, while transcripts from *Actinobacteria* decreased between study days zero and 12 (Fig 3).

Between days 12 and 58, 90% of the topmost upregulated genes were associated with the COG translation, ribosomal structure and biogenesis and all were taxonomically associated with *Betaproteobacteria* (Fig 3A,B). Many of these genes were annotated as proteins within the *rpl* protein family, involved in ribosomal binding. Genes across multiple COG categories with taxonomic associations to *Bacilli* and *Clostridia* decreased

between study days 12 and 58, six of which were transcripts that previously increased
between days zero and 12 (Fig 3B, Supplementary Material 6).

Multiple transcripts associated with the energy production and conversion COG, as
well as transcripts annotated with the COGs inorganic transport and metabolism,
and translation, ribosomal structure and biogenesis, increased between days 58 and
86 (Fig 3A). Two of the upregulated energy and production and conservation tran-
scripts were associated with cytochrome c oxidase subunits in *Betaproteobacteria*,
while another was annotated as *hao*, encoding the enzyme hydroxylamine dehydroge-
nase which is involved in conversion of hydroxylamine to nitrite during nitrification
(Supplementary Material 6). Further investigation into hydroxylamine dehydrogenase
showed a significant increase in *hao* transcripts at day 86 followed by subsequent
decreases at days 168 and 376 ($F = 4.183$; $p = 0.02$). This increase corresponded to
decreased soil ammonium levels and subsequent accumulation of nitrate (Supplemen-
tary Material 1). Half of the topmost downregulated genes between days 58 and 86
were not assigned to a COG (*i.e.*, unclassified) or were of unknown function.

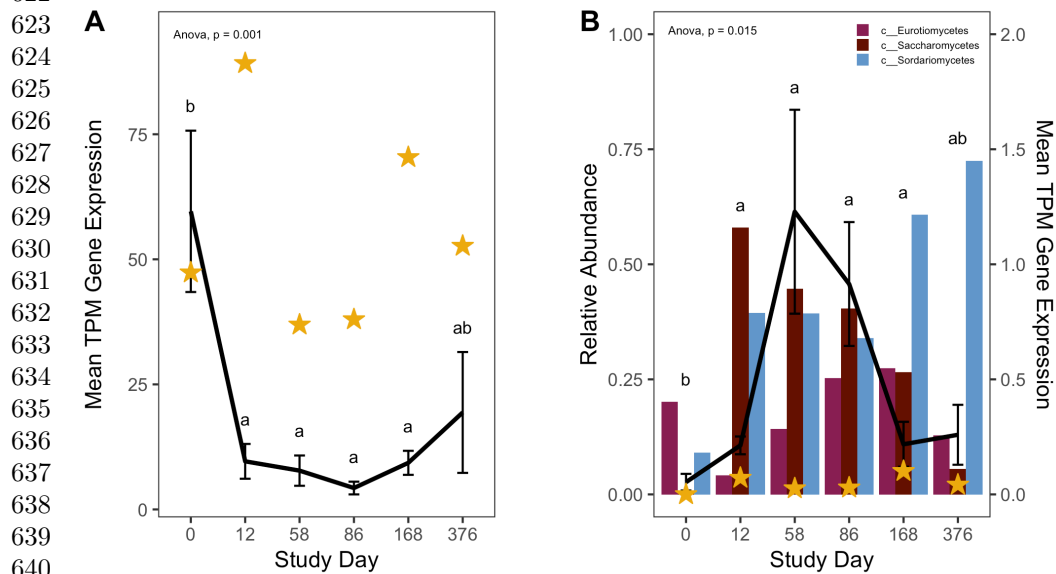
Differential expression comparing study days 86 and 168 and 168 and 376 identi-
fied genes across a variety of functional categories, with many unclassified in the
COG database or with unknown function (Fig 3A). Expression of carbohydrate trans-
port and metabolism genes associated with *Bacilli* decreased between day 168 and
376. Additionally, *Acidobacteria* transcripts increased in decomposition-impacted soils
between study day 168 and 376 (Fig 3B). These transcripts were not associated with
any single COG category, however.

Carbon dominant molecules

We expected to observe increased expression of lipid metabolizing genes during active
and advanced decomposition as microbes degrade lipids deposited in the soil [21].

Therefore, we investigated changes in triacylglycerol lipase (enzyme commission number: 3.1.1.3) gene transcription in our soils. Generally, lipase transcripts decreased as decomposition progressed (HLM $F = 6.564$, $p < 0.001$), however we also observed a significant interaction between study day and taxonomic annotation ($F = 8.786$; $p < 0.001$). Specifically, lipase gene transcripts annotated as bacteria decreased with decomposition time ($F = 10.392$; $p = 0.001$), while fungal lipase transcripts increased, reaching a maximum at study day 58 ($F = 4.509$; $p = 0.015$) (Fig 4).

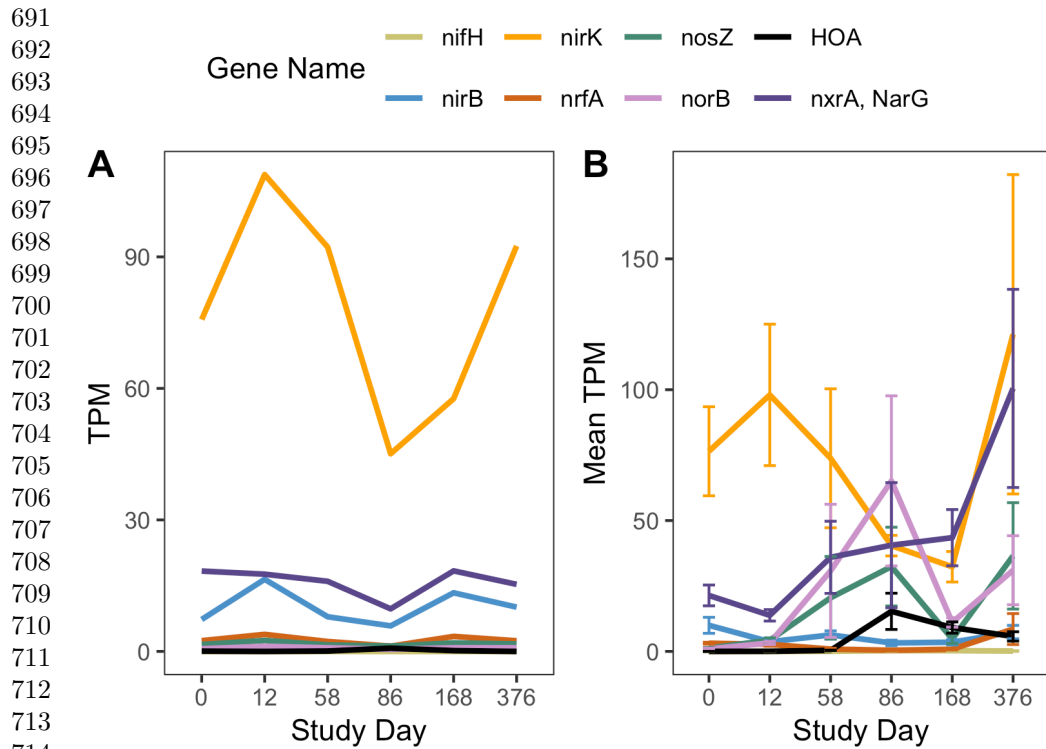
Figure 4: Mean transcript abundance, in transcripts per million (TPM), of all bacterial (A) and fungal (B) triacylglycerol lipase (EC 3.1.1.3) genes over time. Black lines (A, B) report mean and standard deviation of TPM from three individuals (black line), while gold stars denote mean TPM in control soils. P-values are the result of ANOVAs where average TPM and study day are the dependent and independent variables, respectively, while letters are the result of post-hoc Tukey tests between decomposition timepoints. In B, bars show the relative abundance of the fungal classes *Saccharomycetes*, *Sordariomycetes*, and *Eurotiomycetes*, reported in Taylor et al. (2024).



Nitrogen and sulfur enriched molecules

Expression of nitrogen cycling genes was impacted in response to human decomposition. Due to the detection of *hao* in our differential expression analysis, and our hypotheses predicting changes to nitrogen transformation processes, the expression of genes encoding common enzymes involved in nitrogen cycling (*nifH*, *nirB*, *nirK*, *norB*, *nosZ*, *nrfA*, *nrrA*, and *amoA*) were assessed using their enzyme commission numbers (Fig 5A,B). *nifH*, encoding a subunit of nitrogenase which is involved in nitrogen fixation, displayed little to no changes in gene expression between control and decomposition soils. Transcripts for two genes encoding enzymes contributing to the last two steps of denitrification, *norB* (encodes nitric oxide reductase) and *nosZ* (encodes nitrous oxide reductase), increased between study days 12 and 86, and decreased at study day 168 before increasing again at day 376. In contrast, expression of genes encoding nitrate reductase, *narG*, and NO-forming nitrite reductase, *nirK*, remained low until day 376 when transcripts for both genes increased. As noted above, expression of *hao*, encoding hydroxylamine dehydrogenase, increased at study day 86 before decreasing at remaining timepoints (Fig 3A, Fig 5B). Expression of *amoA*, encoding a subunit of ammonia monooxygenase, and *nrrA*, encoding a subunit of nitrite oxidoreductase, which are involved in nitrification, changed in response to decomposition. *amoA* transcripts initially decreased at day 12, remaining reduced until study day 376. Similarly, abundance of genes that encode for enzymes involved in dissimilatory nitrate reduction, *nirB*, and *nrfA*, was low for the first 168 days, with *nrfA* expression increasing at day 376 (Fig 5B).

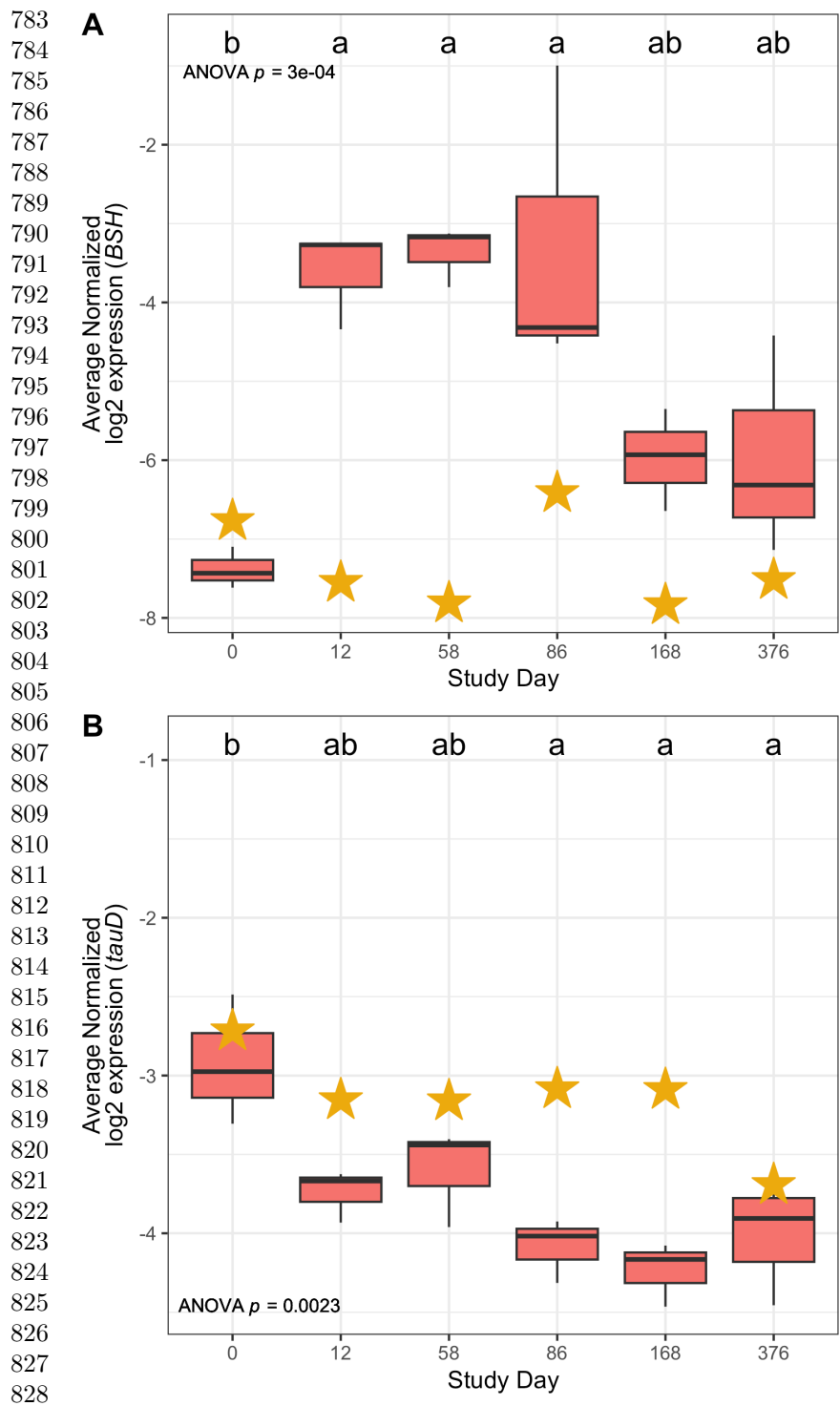
Figure 5: Average gene expression, in transcripts per million (TPM), of commonly used marker genes for enzymes involved in nitrogen cycling over time in controls (A) and decomposition (B) soils. Data in B represent mean and standard deviation of TPM from three individuals.



Expression of genes involved in metabolism of nitrogen and sulfur-containing compounds were also impacted by human decomposition. Specifically, four of the top ten genes whose expression decreased at day 12 were related to taurine metabolism, with their annotations associated with *tauD*, encoding taurine dioxygenase. (Supplementary Material 6). Further investigation into *tauD* showed that mean expression of these genes decreased steadily over one year, beginning at day 12 (Fig 6B); however, *tauD* expression in response to human decomposition was variable across taxonomic associations. Most *tauD* transcripts were associated with *Gammaproteobacteria*, *Actinobacteria*, *Betaproteobacteria*, *Alphaproteobacteria*, and fungi. While a majority of the *tauD* gene queries displayed reduced expression over time, expression of fungal-associated and a few *Betaproteobacteria*-associated *tauD* genes increased at day 58 (Supplementary Material 7). Sources of taurine in the human body include taurine

absorbed from the diet and taurine produced from anaerobic microbial deconjugation of bile salts via bile salt hydrolase (BSH) enzymes [22]. Therefore, we also looked at expression of genes encoding BSH enzymes in decomposition soils. Expression of these genes was elevated at days 12, 58, and 86 before converging toward pre-decomposition levels at days 168 and 376 (Fig 6A). Hierarchical liner mixed effects (HLM) models showed that both *tauD* (HLM $F = 7.356$, $p = 0.002$) and BSH ($F = 13.768$, $p < 0.001$) gene expression was significantly different over time (Fig 6A,B).

Figure 6: Mean bile salt hydrolase, BSH, (A) and *tauD*, taurine dioxygenase, (B) log2 normalized expression in controls (gold stars) and decomposition (boxplots) soils. Boxplots display the 25th and 75th quartiles and median log2 normalized values between all three individuals at each timepoint. ANOVA p-value is the result of a hierarchical linear mixed effects model accounting for repeated measures of each donor block, while letters denote the results of *post-hoc* Tukey test.



Discussion

The goal of this study was to assess soil microbial gene expression in response to human decomposition. Metatranscriptomics were applied to soil samples collected over one-year from below three decomposing human bodies. From this, we showed that microbial gene expression shifted over time, with samples reproducible between individuals. Additionally, we showed that gene expression profiles had not recovered to pre-decomposition conditions after one year. Comparison of control and decomposition expression profiles revealed that heat-shock proteins were elevated in response to decomposition. We also described expression patterns between decomposition timepoints, noting changes in functional gene categories at certain timepoints, in particular with respect to lipid, nitrogen and sulfur metabolism.

Gene expression patterns in decomposition soils

Gene expression profiles remained altered after one year of decomposition. It is unclear if soil microbial communities, in terms of gene expression profiles, have reached a new steady state as a result of decomposition, or if they would eventually return to pre-decomposition conditions. **Stacy, please add sentence to put these results into context of soil chemistry impacts reported in the 2024 pub.** Barton et al. (2020) [23] reported that soil phosphorus, nitrogen (total, ammonium, and nitrate), and electrical conductivity were still elevated above background levels after 500 days of human decomposition, suggesting decomposition events have long lasting effects on the local ecosystem. This has implications for terrestrial ecosystem processing (*e.g.*, nutrient cycling, emission of greenhouse gasses, etc.), as we show that decomposition alters functional metabolism pathways within soil microbial communities. Further work with extended sample collections beyond one year are needed to address how long microbial gene expression is impacted.

Bacteria, fungi, and archaea were all represented in expressed genes throughout decomposition, suggesting that members of all three domains have the potential to contribute to decomposition processes and nutrient cycling. While a majority of annotated transcripts were identified as bacteria, fungal transcripts were the second most abundant group. Fungal transcripts made up almost half (seven of the top 15) of the significantly differentially expressed genes associated with decomposition-impacted soils. Additionally, with respect to expression shifts between decomposition time-points, fungal transcripts were among the topmost upregulated genes at study day 86. The presence of fungal transcripts is not surprising as fungi are key decomposers, involved in the degradation of organic matter in terrestrial ecosystems [24]. It was interesting to see an increase in certain fungal transcripts, such as lipase, at study days 58 and 86 when soil oxygen began to recover, suggesting that fungal activity in decomposition soils may be constrained by altered oxygen levels. Similarly, prior work with these soils showed a relationship between fungal community composition and soil oxygen [17], indicating that fungal communities underwent shifts in both community structure and activity in decomposition-impacted soils.

Heat-shock/stress response

Soil microbial communities expressed stress response genes in response to human decomposition. Differential expression analysis identified increased expression of multiple heat shock proteins associated with the taxa *Xanthomonadales*, *Actinobacteria*, and fungi. Upon further investigation, expression of these genes increased through day 58 and remained high for the remainder of the year. Soil temperature was elevated relative to controls (up to 10°C higher) between study days 12 and 100, while soil electrical conductivity increased up to 663 $\mu\text{S}/\text{cm}$ (16X higher than background) through day 58 before slowly decreasing through the remainder of the study. Soil electrical conductivity, which correlates with ionic strength [25] and can indicate soil

salinity, has previously been shown to increase in decomposition soils [8–10, 17]. As a result, we would expect these microbes to be experiencing both heat and osmotic stress during this period. Prior work has observed increased heat shock gene expression during salt stress in paddy soils [26] and the presence of both heat and osmotic stress genes in desert soils along a salt gradient [27], suggesting saline conditions can alter the expression of heat and/or osmotic stress genes. In our study we observed that soil microbial communities elicit a stress response during human decomposition, however, at this time, it is unclear if expression of these genes is in response to heat stress alone, or in combination with osmotic stress.

Carbon-containing compounds

Humans fat tissue contains lipids that are broken down during decomposition. Therefore, we assessed expression of triacylglycerol lipase genes in decomposition soils. Our results show that expression of triacylglycerol lipase genes was altered in response to decomposition, and these shifts differed between bacterial and fungal transcripts. Bacterial triacylglycerol lipase transcripts decreased in response to decomposition, while fungal triacylglycerol lipase transcripts increased. These results suggest that fungi may be important triacylglycerol degraders in human decomposition-impacted soils. Further, expression of these genes was correlated to the relative abundance of the fungal classes *Saccharomycetes*, *Sordariomycetes*, and *Eurotiomycetes* [17]. These fungi have been previously associated with decomposition soils [14, 16] and are known to contain triacylglycerol lipase genes in their genomes [28, 29], suggesting that these organisms are important for lipid degradation in decomposition soils.

Our observation of an overall decrease in triacylglycerol lipase transcripts contrasts with previous work by Howard et al. (2010) [21], who observed increased gene copy number of Group 1 lipase genes via qPCR during swine decomposition. Fatty acid composition differs in human compared to pig tissue [30], potentially altering the

lipid profile available for microbes, leading to differences in decomposition products within the soil [20]. These products can then directly or indirectly alter community composition and/or activity of functional proteins via substrate availability or the chemical environment. Further, decomposition of humans and pigs resulted in increased pH in soils below pigs, and decreased pH below humans [20]. Altered pH and soil chemistry could result in a different functional potential and/or gene expression in decomposition-impacted soils, especially as it relates to lipase genes, as many triacylglycerol lipases have a pH optimum that is neutral to basic [31–33], so cells may be decreasing expression under acidic conditions in human decomposition soils. Availability of lipid species and changes to pH may select for taxa that favor these substrates/pH conditions; for example, Mason et al. (2022) [34] suggested the abundance of the fungal taxa *Saccharomycetes* was related to antemortem BMI due to relative proportions of fat and muscle tissue.

Nitrogen enriched compounds/N-cycling

The human body is a concentrated source of nitrogen that is released into the surrounding soil during decomposition, therefore we also evaluated expression of genes involved in nitrogen cycling. Expression of common marker genes for nitrogen cycling was altered in decomposition soil and suggested nitrogen transformations during human decomposition are driven by soil oxygen concentrations with hydroxylamine as an important intermediate. We observed low or reduced expression of nitrification genes *nxrA* and *amoA* between days 12 and 86, during a period when oxygen was reduced to 39% - 85%. This was concomitant with accumulation of ammonium, which reached a maximum on day 12, and low nitrate conditions indicating that nitrification was inhibited. This period of reduced soil oxygen constraining nitrification was also described in a decomposition experiment with beaver carcasses Keenan et al. (2018) [8].

We observed increased expression of *hao*, which encodes the enzyme hydroxylamine
 dehydrogenase (HAO) at day 86 while oxygen was reduced (~85%). This corresponded
 to simultaneous increases in expression of genes encoding nitric oxide reductase (*norB*)
 and nitrous oxide reductase (*nosZ*). Traditionally HAO has been thought to pro-
 cess hydroxylamine to nitrite during nitrification, while NorB and NosZ are enzymes
 involved in the last two steps of denitrification converting nitric oxide (NO) to dini-
 trogen gas (N₂). However, recent work has suggested hydroxylamine can be converted
 to nitric oxide (NO), as well as can interact with multiple phases of the nitrogen cycle
 [35]. Even though *amoA* expression was shown to decrease during reduced oxygen
 conditions, *amoA* transcripts were still present and likely able to convert ammonium
 to hydroxylamine as soil oxygen was not completely depleted during decomposition.
 Additionally, a previous study reported that the growth of the ammonia oxidizing
 bacteria *Nitrosomonas europaea* under anoxic conditions lead to accumulation of
 hydroxylamine in a chemostat bioreactor [36], suggesting anaerobic ammonium oxi-
 dation (anammox) may also be occurring in decomposition soils. However, we did
 not observe increases in *nirK* expression, which might suggest conversion of nitrite to
 NO for use in the anammox pathway. NO produced via HAO activity may be used
 for anammox in these soils; however, the role of hydroxylamine as an intermediate
 in anammox is still debated [35]. Therefore, our current hypothesis is that hydroxy-
 lamine accumulates under anaerobic conditions during decomposition, which can then
 be converted to NO by HAO. This NO would then be present for anaerobic denitri-
 fying bacteria to convert to nitrous oxide (N₂O) by NorB and finally to N₂ by NosZ.
 Keenan et al. (2018) [8] also noted a brief increase in N₂O emissions, which suggests
 denitrification was occurring during this phase of reduced soil oxygen concentrations.
 As soils fully reoxygenated by day 168, we observed increased expression of genes
 encoding enzymes involved in aerobic nitrification, *amoA* and *nxrR*. Nitrification is
 an oxygen-dependent process which would be converting the accumulated ammonium

to nitrate; the increase in nitrate concentrations may then serve as a substrate for denitrification. We observed increased expression of marker genes encoding all four enzymes in the complete dissimilatory denitrification pathway (*narG*, *nirK*, *norB*, and *nosZ*) at day 376. Increased expression of nitrification and denitrification marker genes is consistent with accumulation of nitrite, nitrate, and N₂O after oxygen is reintroduced to soils described in Keenan et al. (2018) [8]. Together, gene expression patterns in our study provide further insight into nitrogen transformations in during vertebrate decomposition, suggesting an important role of hydroxylamine.

Sulfur-containing compounds

Sulfur is present in various organic molecules, including taurine, a sulfur- and nitrogen-containing acid involved in bile acid formation [22]. Taurine is present in the human body, where it can be absorbed from the diet or synthesized in the liver [37]. However, taurine is also produced as a byproduct of the deconjugation of bile salts via bile salt hydrolases (BSH) present in the anaerobic gut taxa *Lactobacillus* and *Clostridium* [22]. In our study, we observed increased expression of genes encoding BSH enzymes between days 12 and 86. Given that increased expression of BSH genes corresponded to the beginning of active decomposition, when decomposition products were observed to enter the soil, and the period of reduced dissolved oxygen in our study, it is likely that taurine accumulation is the result of BSH enzyme activity by anaerobic microorganisms. While we did not measure taurine concentrations in this study, our results correspond to previous decomposition studies that report accumulation of taurine in various organs and body regions [38–40] and soils [20, 41] during decomposition via metabolomics, and increased relative abundance of *Clostridium* and *Lactobacillus* within the body [42–44] and in decomposition soils [11] via DNA sequencing methods, including in these soils [17].

One pathway of taurine metabolism is through desulfurization via the α -ketoglutarate-dependent enzyme taurine dioxygenase (TauD). Specifically, this enzyme, encoded by the gene *tauD*, converts 2-oxoglutarate and taurine to produce aminoacetaldehyde, succinate, sulfite, and CO₂ [45]. Succinate and sulfite from this reaction can then be used for the citric acid cycle and sulfur metabolism, respectively. Given increased BSH expression in our study and reported taurine accumulation in others, we would expect taurine to be present for microbial metabolism by TauD. However, we observed a general decrease in *tauD* expression between days 12 through 376. This trend was driven by reduced expression of *tauD* transcripts associated with *Proteobacteria*, *Gammaproteobacteria*, and *Actinobacteria* whose relative abundance have been shown to remain consistent or increase during human decomposition [11], suggesting that *tauD* expression is downregulated under decomposition conditions. However, we noted that expression of *tauD* genes associated with fungi and a few *Betaproteobacteria* displayed increased expression at day 58, corresponding to increased expression of bile salt hydrolases (BSH) between days 12 and 86. The reduction in *tauD* expression may be due to sulfur availability. We did not measure sulfur species in this experiment; however, others have observed increased sulfur concentrations in decomposition-impacted soils [3, 7, 46]. Thus, sulfur scavenging pathways such as taurine desulfurization by TauD [47], whose genes are expressed under sulfur-limiting conditions, likely display reduced expression under sulfur replete conditions. Additionally, taurine may be processed through other pathways. For example, taurine can be deaminated by taurine dehydrogenase to produce sulfite and acetyl-CoA for carbon metabolism [45, 48]. Overall, our results suggest that human decomposition has potential impacts on soil sulfur biogeochemistry through deposition of inorganic (sulfate) and organic (sulfur-containing amino acids) sulfur compounds.

1151 **Conclusion**

1152

1153 This study represents the first investigation of soil microbial gene expression dur-
1154 ing human decomposition. Metatranscriptomic analysis of soils from three human
1155 individuals over one year shows that decomposition impacted microbial community
1156 gene expression profiles, exhibiting functional shifts over time. This included altered
1157 expression of genes involved in lipid, N and S metabolism as microbes processed
1158 the nutrient-rich tissues of the human body. Additionally, we noted that function-
1159 ality within decomposition-impacted soils was still affected after one year and had
1160 not returned to starting or background conditions. Together, these results show that
1161 vertebrate decomposition has lasting impacts on local soil ecosystems, including soil
1162 microbial communities. These results have important implications for understanding
1163 biogeochemical changes due to vertebrate mortality events in terrestrial ecosystems.
1164

1171

1172

1173 **Materials and Methods**

1174

1175

1176 **Study design**

1177

1178 In February 2018, three deceased male human subjects (hereafter, “donors”) were
1179 placed supine on the soil surface at the University of Tennessee Anthropology Research
1180 Facility (ARF) and allowed to decompose. Located in Knoxville, TN (35° 56’ 28” N,
1181 83° 56’ 25” W) the ARF is a roughly 2-acre outdoor facility dedicated to studying
1182 human decomposition [12]. The soils at the ARF are comprised of the Loyston-Talbott-
1183 Rock outcrop (LtD) and Coghill-Corryton (CcD) complexes. LtD soils are a silty clay
1184 loam and channery clay overlaying lithic bedrock, while CcD soils are comprised of
1185 clay from weathered quartz limestone [12, 17]. A site that had not been previously
1186 exposed to decomposition was used for this study.
1187

1193

1194 The decomposition field experiment is fully described in Taylor et al. (2024) [17].

1195

1196 Briefly, experiments were conducted in a block design, where each block consisted of

one decomposition site and one control site [17]. In total three blocks, *i.e.*, three donors paired with three respective control sites, were included in the study. Each control site was chosen in a manner to ensure their location was uphill and roughly 2 m away from decomposition sites [17]. Donor internal temperatures were recorded by probes located in the abdomen, while ambient air temperatures were monitored via sensors located roughly 50 cm above the soil surface. Soil temperature and salinity were measured with sensors placed directly underneath each individual (Decagon Devices, GS3) [17]. Donor ages ranged from 65 to 86 and were within 1 kg of each other with regard to weight (90.7 to 91.6 kg); donor BMI varied between 27.7 to 29.6 [17].

Sampling and physiochemistry

Decomposition of all subjects was observed for one year. During the one-year study period, soils were sampled at 20 timepoints chosen to correspond with morphological stages of decomposition as described by [49]. Once advanced decay was reached, soils were collected at intervals of 350 accumulated degree days (ADD), calculated using ambient air temperatures, up to one year. All soil cores were taken using a 1.9 cm (3/4 inch) diameter soil auger to a depth of 16 cm. Soil cores were sub-fractioned in to 0 to 1 cm and 1 to 16 cm for the analyses reported in Taylor et al. (2024) [17]; the entire 0 to 16 cm core was used for this current study. Decomposition soils were taken from directly beneath the cadavers, taking care to not re-sample the same location more than once. At the time of sampling, soil dissolved oxygen was measured in triplicate using an Orion Star™ A329 pH/ISE/Conductivity/Dissolved Oxygen portable multiparameter meter (ThermoFisher) [17].

A subset of 6 study timepoints were chosen for metatranscriptomics analysis. Study days 0, 12, 58, 86, 168, and 376 were chosen as they represented distinct morphological and soil biogeochemical stages during decomposition. Study day 0 was chosen as a baseline sample prior to cadaver placement. Study day 12 was chosen as this was they

1243 start of active decomposition and corresponded to maximum soil ammonium concen-
1244 trations and minimum soil oxygen (approximately 39%). Study day 58 was chosen
1245 as this sample represented the pH minimum, and respirationn and soil temperature
1246 were at a maximum [17]. Additionally, ammonium concentrations began to decrease
1247 around day 58. Study day 86 was chosen as the time period when soil oxygen started
1248 to recover and nitrate levels began to increase. Study day 168 was chosen as nitrate
1249 was at its maximum and soil dissolved oxygen had returned to 99%. Finally, day 376
1250 was chosen to represent the end of the study, approximately 1 year since cadaver pal-
1251 cement. Each study day was represented by four soil samples for RNA extraxtion: one
1252 pooled control sample which was a mix of the three control locations, plus one sample
1253 from each of the three donors, yielding a total of 24 samples for this study.

1261
1262 Soil samples were transported back to the lab at the University of Tennessee
1263 (Knoxville, TN) and processed within 24 hours of collection. Soils were homogenized
1264 by hand to remove insect larvae, roots, rocks, and other debris (> 2 mm). A subset
1265 of soils were used to measure pH, electrical conductivity (EC), and evolved CO_2 as
1266 described in Taylor (2020). Soil nitrogen species (NH_4^+ , NO_3^-) and total carbon (TC)
1267 and nitrogen (TN) were measured in all soil samples as described in [17]. Roughly 10
1268 g of soil was reserved for nucleic acid extraction, placed in a 4 oz. Whirl-Pak™ bag
1269 (Nasco), and flash frozen in liquid nitrogen. All samples were stored at -80°C until fur-
1270 ther analysis. Bacterial and fungal community composition was assessed via amplicon
1271 sequencing of the 16S rRNA gene and ITS2 region as described in Taylor et al. (2024).

1280 RNA Extraction and Sequencing

1281
1282 RNA was extracted from 2 g of soil using Qiagen's RNeasy® PowerSoil® Total RNA kit
1283 (catalog no. 12866-25). Manufacturer's instructions were followed with a few modifica-
1284 tions. Soils became saline during decomposition; therefore, we followed manufacturer's
1285 suggestion and incubated all extracts at -20°C following addition of solution SR4 (step
1286
1287
1288

9) to decrease salt precipitation. All RNA samples were resuspended in 40 µl of Solution SR7. RNA concentrations were assessed fluorometrically using the Qubit® RNA HS assay (catalog no. Q32852) with 1 µl of RNA. DNA contamination was removed by DNase treating RNA extracts twice using Qiagen’s DNase Max® kit in 50 µl reactions. RNA concentrations were remeasured after DNase treatment. PCR with general V4 16S rRNA gene primers [50, 51] was conducted using RNA extracts as the template to confirm removal of all DNA prior to sequencing. RNA aliquots were shipped to HudsonAlpha Discovery (Huntsville, AL) for library preparation and RNA sequencing. Dual-indexed libraries were prepared using the Illumina® Stranded Total RNA prep with ribosomal RNA depletion via ligation with Ribo-Zero Plus. Libraries were then pooled and sequenced on Illumina’s NovaSeq 6000 v4 platform, resulting in demultiplexed fastq files for each sample.

Bioinformatics

Read quality control (QC) was conducted in KBase [52] using Trimmomatic [53]. Paired fastq files were imported to KBase through Globus. Poor quality reads were removed, and adapters trimmed via Trimmomatic (v0.36) using default settings and the TruSeq3-PE-2 adapter file. After QC check with FastQC, trimmed libraries were exported as fastq files from KBase through Globus. Remaining ribosomal RNA was filtered using bbmap (maxindel = 20, minid = 0.93) from the Joint Genome Institute’s (JGI) bbtools suite [54]. After this step, all non-ribosomal reads from all 24 samples were merged into one file. This file was then used to co-assemble reads into contigs using the de novo assembler MEGAHIT (v1.2.9) [55] (−12 −k-min 23, −k-max 123, −k-step 10).

Gene identification and annotation from co-assembled contigs was performed using Prodigal [56] and eggNOG mapper [57], respectively. Briefly, the fastq containing all contigs was submitted to Prodigal (v2.6.3) for protein coding gene predication for

a meta-sample (-p meta -f gff). Next, predicated genes were functionally and taxonomically annotated using eggNOG mapper (v2.1.6) using basic settings to perform a diamond blastp search [58]. Only genes that were both functionally and taxonomically annotated by one of the databases used by eggNOG mapper and identified as bacterial, archaeal, or fungal were chosen as genes of interest. Transcript counts for all genes of interest were obtained by mapping reads from each respective sample to genes of interest obtained from co-assembly using QIAGEN CLC Genomics Workbench 20.0 (<https://digitalinsights.qiagen.com/>).

Differential Expression

Transcript counts from all samples were combined in a single workable data file and imported into R for differential expression analysis using the R packages edgeR [59] and limma [60] following a modified pipeline by Phipson et al. (2020) [61]. Briefly, the transcript count table was imported into R and converted to a DGEList object. Genes without sufficient counts for statistical analysis were removed to increase power using the edgeR function filterByExpr(). Raw counts were then log2 normalized and gene expression profiles compared via multidimensional scaling (MDS) and hierarchical clustering. For differential expression analysis, raw filtered reads were normalized using edgeR's trimmed mean of M values (TMM) normalization using the function calcNormFactors(). TMM normalized reads were then log2 transformed using limma's voom() and differential expression assessed. Empirical Bayes shrinkage was used correct to p-values for false discovery rates. The topmost up and down regulated genes for each comparison, determined by log2 fold change and adjusted p-values, were then reported. Expression of certain genes were assessed after performing transcripts per million (TPM) normalization and statistical analyses with a combination of analysis of variance (ANOVA) and post-hoc Tukey tests. ANOVA across all timepoints were applied to hierarchical linear mixed effects models to account for repeated sampling within each donor block.

Availability of data and materials

RNA sequence files from the Novoseq instrument can be found at XXXX. The datasets supporting the conclusions of this article are available at the GitHub repository [Mason_MetaT_XXX_2024](#).”

References

[1] Benninger, L. A., Carter, D. O. & Forbes, S. L. The biochemical alteration of soil beneath a decomposing carcass. *Forensic Sci Int* **180**, 70–5 (2008).

[2] Towne, E. G. Prairie vegetation and soil nutrient responses to ungulate carcasses. *Oecologia* **122**, 232–239 (2000). URL <https://doi.org/10.1007/PL00008851>.

[3] Taylor, L. S. *et al.* Soil elemental changes during human decomposition. *PLOS ONE* **18**, 1–24 (2023). URL <https://doi.org/10.1371/journal.pone.0287094>. Publisher: Public Library of Science.

[4] Parmenter, R. R. & MacMahon, J. A. Carrion decomposition and nutrient cycling in a semiarid shrub–steppe ecosystem. *Ecological Monographs* **79**, 637–661 (2009).

[5] Macdonald, B. C. T. *et al.* Carrion decomposition causes large and lasting effects on soil amino acid and peptide flux. *Soil Biology and Biochemistry* **69**, 132–140 (2014).

[6] Bump, J. K. *et al.* Ungulate Carcasses Perforate Ecological Filters and Create Biogeochemical Hotspots in Forest Herbaceous Layers Allowing Trees a Competitive Advantage. *Ecosystems* **12**, 996–1007 (2009).

[7] Aitkenhead-Peterson, J. A., Owings, C. G., Alexander, M. B., Larison, N. & Bytheway, J. A. Mapping the lateral extent of human cadaver decomposition with soil chemistry. *Forensic Sci Int* **216**, 127–34 (2012).

1427 [8] Keenan, S. W., Schaeffer, S. M., Jin, V. L. & DeBruyn, J. M. Mortality hotspots:
1428
1429 nitrogen cycling in forest soils during vertebrate decomposition. *Soil Biology and*
1430 *Biochemistry* **121**, 165–176 (2018).
1431
1432
1433 [9] Fancher, J. P. *et al.* An evaluation of soil chemistry in human cadaver decom-
1434 position islands: Potential for estimating postmortem interval (PMI). *Forensic*
1435 *Science International* **279**, 130–139 (2017).
1436
1437
1438 [10] Quaggiotto, M.-M., Evans, M. J., Higgins, A., Strong, C. & Barton, P. S.
1439 Dynamic soil nutrient and moisture changes under decomposing vertebrate
1440 carcasses. *Biogeochemistry* **146**, 71–82 (2019).
1441
1442
1443 [11] Cobaugh, K. L., Schaeffer, S. M. & DeBruyn, J. M. Functional and structural
1444 succession of soil microbial communities below decomposing human cadavers.
1445 *Plos One* **10**, e0130201 (2015).
1446
1447
1448 [12] Keenan, S. W. *et al.* Spatial impacts of a multi-individual grave on microbial
1449 and microfaunal communities and soil biogeochemistry. *Plos One* **13**, e0208845
1450 (2018).
1451
1452
1453 [13] Singh, B. *et al.* Temporal and spatial impact of human cadaver decomposition on
1454 soil bacterial and arthropod community structure and function. *Front Microbiol*
1455 **8**, 2616 (2018).
1456
1457
1458 [14] Metcalf, J. L. *et al.* Microbial community assembly and metabolic function during
1459 mammalian corpse decomposition. *Science* **351**, 158–62 (2016).
1460
1461
1462 [15] Finley, S. J., Pechal, J. L., Benbow, M. E., Robertson, B. K. & Javan, G. T.
1463 Microbial Signatures of Cadaver Gravesoil During Decomposition. *Microb Ecol*
1464 **71**, 524–529 (2016).
1465
1466
1467
1468
1469
1470
1471
1472

- [16] Fu, X. *et al.* Fungal succession during mammalian cadaver decomposition and potential forensic implications. *Sci Rep* **9**, 12907 (2019). 1473
1474
1475
1476
- [17] Taylor, L. S. *et al.* Soil microbial communities and biogeochemistry during human decomposition differs between seasons: evidence from year-long trials (2024). 1477
1478
1479
URL <https://www.researchsquare.com/article/rs-3931135/v1>. 1480
1481
1482
- [18] Burcham, Z. M. *et al.* Total RNA analysis of bacterial community structural and functional shifts throughout vertebrate decomposition. *J Forensic Sci* **64**, 1483
1484
1485
1707–1719 (2019). 1486
1487
1488
- [19] Ashe, E. C., Comeau, A. M., Zejdlik, K. & O’Connell, S. P. Characterization of bacterial community dynamics of the human mouth throughout decomposition 1489
1490
1491
via metagenomic, metatranscriptomic, and culturing techniques. *Front Microbiol* 1492
1493
12, 689493 (2021). 1494
1495
- [20] DeBruyn, J. M. *et al.* Comparative decomposition of humans and pigs: soil 1496
1497
biogeochemistry, microbial activity and metabolomic profiles. *Front Microbiol* 1498
1499
11, 608856 (2021). 1500
1501
- [21] Howard, G. T., Duos, B. & Watson-Horzelski, E. J. Characterization of the 1502
1503
soil microbial community associated with the decomposition of a swine carcass. 1504
1505
International Biodeterioration & Biodegradation **64**, 300–304 (2010). 1506
1507
- [22] Urdaneta, V. & Casadesús, J. Interactions between Bacteria and Bile Salts in 1508
1509
the Gastrointestinal and Hepatobiliary Tracts. *Frontiers in Medicine* **4** (2017). 1510
1511
- [23] Barton, P. S. *et al.* Soil chemical markers distinguishing human and pig decomposition islands: a preliminary study. *Forensic Science, Medicine and Pathology* 1512
1513
1514
(2020). 1515
1516
1517
1518

1519 [24] van der Wal, A., Geydan, T. D., Kuyper, T. W. & de Boer, W. A thready affair:
1520 linking fungal diversity and community dynamics to terrestrial decomposition
1521 processes. *Fems Microbiology Reviews* **37**, 477–494 (2013).
1522
1523
1524
1525 [25] Essington, M. E. *Soil and water chemistry: an integrative approach* (CRC press,
1526 2015).
1527
1528
1529 [26] Peng, J., Wegner, C.-E. & Liesack, W. Short-Term Exposure of Paddy Soil Micro-
1530 bial Communities to Salt Stress Triggers Different Transcriptional Responses of
1531 Key Taxonomic Groups. *Frontiers in Microbiology* **8** (2017).
1532
1533
1534
1535 [27] Pandit, A. S. *et al.* A snapshot of microbial communities from the Kutch: one of
1536 the largest salt deserts in the World. *Extremophiles* **19**, 973–987 (2015).
1537
1538
1539 [28] Dujon, B. *et al.* Genome evolution in yeasts. *Nature* **430**, 35–44 (2004).
1540
1541
1542 [29] Haridas, S. *et al.* The genome and transcriptome of the pine saprophyte *Ophios-*
1543 *toma piceae*, and a comparison with the bark beetle-associated pine pathogen
1544 *Grosmannia clavigera*. *BMC Genomics* **14**, 373 (2013).
1545
1546
1547 [30] Notter, S. J., Stuart, B. H., Rowe, R. & Langlois, N. The Initial Changes of
1548 Fat Deposits During the Decomposition of Human and Pig Remains. *Journal of*
1549 *Forensic Sciences* **54**, 195–201 (2009).
1550
1551
1552
1553 [31] Kok, R. G. *et al.* Characterization of the extracellular lipase, LipA, of *Acineto-*
1554 *bacter calcoaceticus* BD413 and sequence analysis of the cloned structural gene.
1555 *Molecular Microbiology* **15**, 803–818 (1995).
1556
1557
1558
1559 [32] Hasan, F., Shah, A. A. & Hameed, A. Influence of culture conditions on lipase
1560 production by *Bacillus* sp. FH5. *Annals of Microbiology* **56**, 247–252 (2006).
1561
1562
1563
1564

- [33] Zouaoui, B. & Bouziane, A. Production, optimization and characterization of the lipase from *Pseudomonas aeruginosa*. *Romanian biotechnological letters* **17**, 7187–7193 (2012).
- [34] Mason, A. R. *et al.* Body mass index (BMI) impacts soil chemical and microbial response to human decomposition. *mSphere* **0**, e0032522 (2022).
- [35] Soler-Jofra, A., Pérez, J. & van Loosdrecht, M. C. M. Hydroxylamine and the nitrogen cycle: A review. *Water Research* **190**, 116723 (2021).
- [36] Yu, R., Perez-Garcia, O., Lu, H. & Chandran, K. *Nitrosomonas europaea* adaptation to anoxic-oxic cycling: Insights from transcription analysis, proteomics and metabolic network modeling. *Science of the Total Environment* **615**, 1566–1573 (2018).
- [37] Seidel, U., Huebbe, P. & Rimbach, G. Taurine: A Regulator of Cellular Redox Homeostasis and Skeletal Muscle Function. *Molecular Nutrition & Food Research* **63**, 1800569 (2019).
- [38] Mora-Ortiz, M., Trichard, M., Oregioni, A. & Claus, S. P. Thanatometabolomics: introducing NMR-based metabolomics to identify metabolic biomarkers of the time of death. *Metabolomics* **15**, 37 (2019).
- [39] Locci, E. *et al.* A ¹H NMR metabolomic approach for the estimation of the time since death using aqueous humour: an animal model. *Metabolomics* **15**, 76 (2019).
- [40] Zelentsova, E. A. *et al.* Post-mortem changes in the metabolomic compositions of rabbit blood, aqueous and vitreous humors. *Metabolomics* **12**, 172 (2016).
- [41] Hoeland Katharina, M. *Investigating the potential of postmortem metabolomics in mammalian decomposition studies in outdoor settings*. Ph.D. thesis, University

1611 of Tennessee-Knoxville, https://trace.tennessee.edu/utk_graddiss/7000 (2021).

1612

1613 [42] Javan, G. T. *et al.* Human thanatobiome succession and time since death.

1614 *Sci Rep* **6**, 29598 (2016).

1615

1616

1617 [43] Javan, G. T., Finley, S. J., Smith, T., Miller, J. & Wilkinson, J. E. Cadaver

1618 thanatobiome signatures: the ubiquitous nature of *Clostridium* species in

1619 human decomposition. *Front Microbiol* **8**, 2096 (2017).

1620

1621

1622

1623 [44] DeBruyn, J. M. & Hauther, K. A. Postmortem succession of gut microbial

1624 communities in deceased human subjects. *Peerj* **5**, e3437 (2017).

1625

1626

1627 [45] Cook, A. M. & Denger, K. Metabolism of taurine in microorganisms. *Taurine* **6**

1628 3–13 (2006).

1629

1630

1631

1632 [46] Vass, A. A., Bass, W. M., Wolt, J. D., Foss, J. E. & Ammons, J. T. TIME

1633 SINCE DEATH DETERMINATIONS OF HUMAN CADAVERS USING SOIL

1634 SOLUTION. *Journal of Forensic Sciences* **37**, 1236–1253 (1992).

1635

1636

1637 [47] Kertesz, M. A. Riding the sulfur cycle – metabolism of sulfonates and sulfate

1638 esters in Gram-negative bacteria. *Fems Microbiology Reviews* **24**, 135–175 (2000).

1639

1640

1641 [48] Brüggemann, C., Denger, K., Cook, A. M. & Ruff, J. Enzymes and genes of

1642 taurine and isethionate dissimilation in *Paracoccus denitrificans*. *Microbiology*

1643 (*Reading, England*) **150**, 805–816 (2004).

1644

1645

1646

1647 [49] Payne, J. A. A summer carrion study of the baby pig *Sus Scrofa* Linnaeus.

1648 *Ecology* **46**, 592–602 (1965).

1649

1650

1651

1652 [50] Apprill, A., McNally, S., Parsons, R. & Weber, L. Minor revision to V4 region SSU

1653 rRNA 806R gene primer greatly increases detection of SAR11 bacterioplankton.

1654 *Aquatic Microbial Ecology* **75**, 129–137 (2015).

1655

1656

- [51] Parada, A. E., Needham, D. M. & Fuhrman, J. A. Every base matters: assessing small subunit rRNA primers for marine microbiomes with mock communities, time series and global field samples. *Environmental Microbiology* **18**, 1403–14 (2016).
- [52] Arkin, A. P. *et al.* KBase: The United States Department of Energy Systems Biology Knowledgebase. *Nature Biotechnology* **36**, 566–569 (2018).
- [53] Bolger, A. M., Lohse, M. & Usadel, B. Trimmomatic: a flexible trimmer for Illumina sequence data. *Bioinformatics* **30**, 2114–2120 (2014).
- [54] Bushnell, B. BBMap.
- [55] Li, D., Liu, C.-M., Luo, R., Sadakane, K. & Lam, T.-W. MEGAHIT: an ultra-fast single-node solution for large and complex metagenomics assembly via succinct de Bruijn graph. *Bioinformatics* **31**, 1674–1676 (2015).
- [56] Hyatt, D. *et al.* Prodigal: prokaryotic gene recognition and translation initiation site identification. *Bmc Bioinformatics* **11**, 119 (2010).
- [57] Cantalapiedra, C. P., Hernández-Plaza, A., Letunic, I., Bork, P. & Huerta-Cepas, J. eggNOG-mapper v2: Functional Annotation, Orthology Assignments, and Domain Prediction at the Metagenomic Scale. *Molecular Biology and Evolution* **38**, 5825–5829 (2021).
- [58] Buchfink, B., Reuter, K. & Drost, H.-G. Sensitive protein alignments at tree-of-life scale using DIAMOND. *Nature Methods* **18**, 366–368 (2021).
- [59] Robinson, M. D., McCarthy, D. J. & Smyth, G. K. edgeR: a Bioconductor package for differential expression analysis of digital gene expression data. *Bioinformatics* **26**, 139–140 (2010).

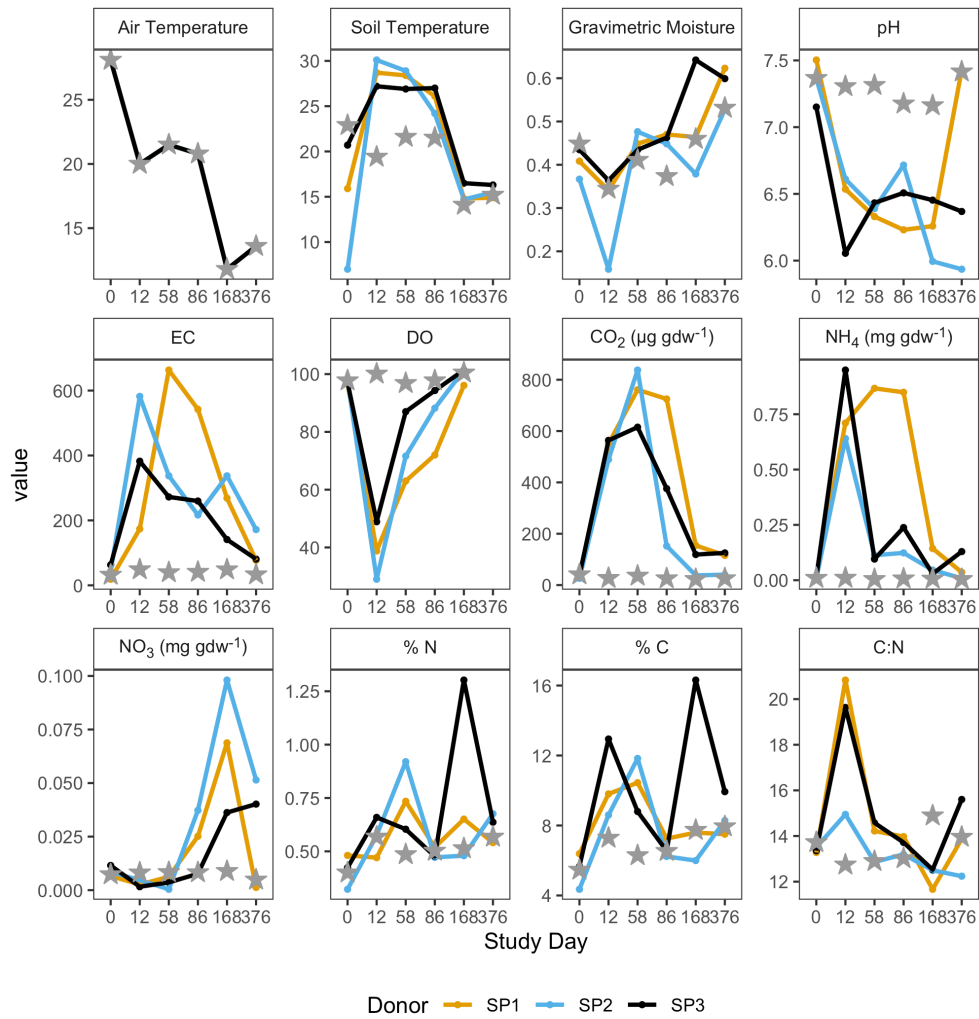
[60] Smyth, G. K. in *limma: Linear Models for Microarray Data* (eds Gentleman, R., Carey, V. J., Huber, W., Irizarry, R. A. & Dudoit, S.) *Bioinformatics and Computational Biology Solutions Using R and Bioconductor* 397–420 (Springer New York, New York, NY, 2005).

[61] Phipson, B. *et al.* Differential expression analysis (2020).

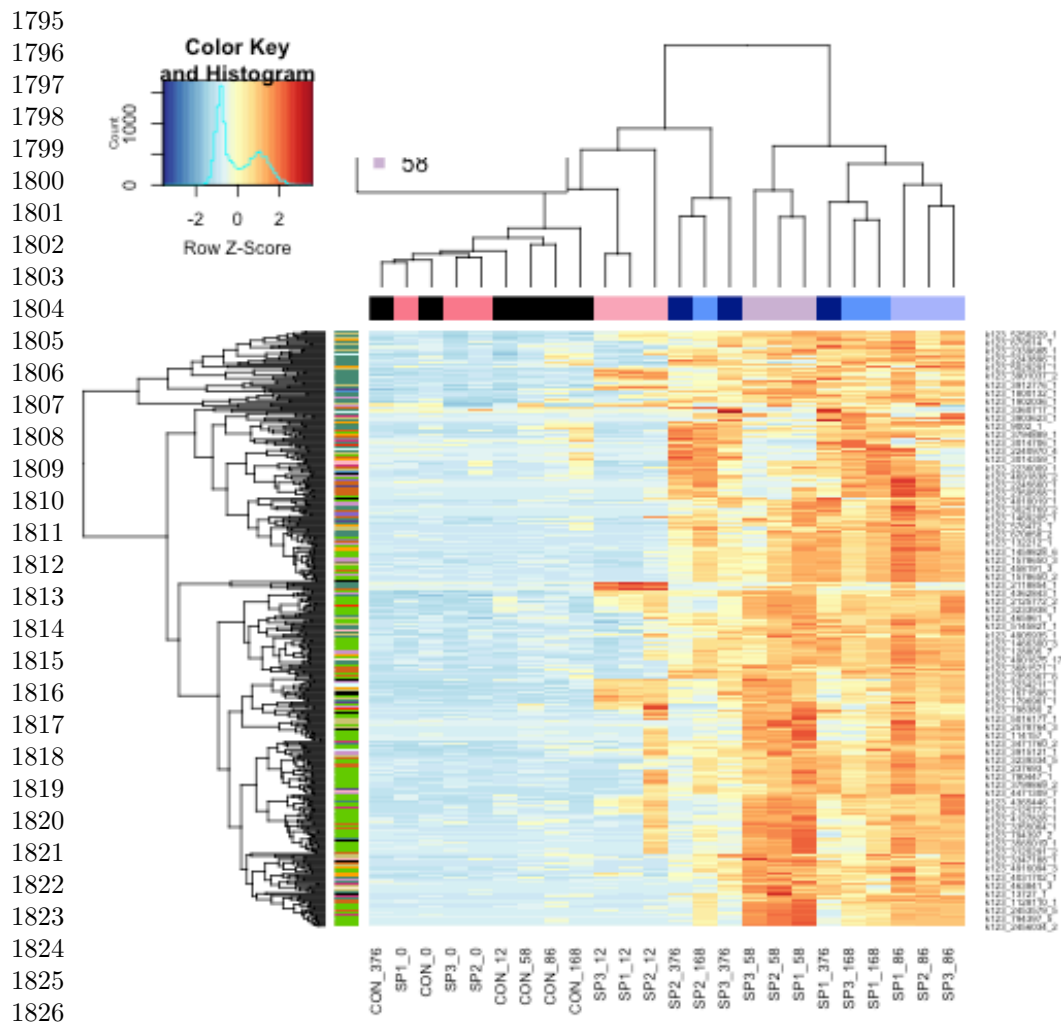
Acknowledgements

We would like to thank the Forensic Anthropology Center at the University of Tennessee-Knoxville for their help in setting up field experiments. We would like to thank Mary Davis for her help in managing the field site and helping to obtain donors for this work. This research was funded by a National Institute of Justice Award (DOJ-NIJ-2017-R2-CX-0008) to LST and JMD.

Supplementary Information



Supplementary Material 1: Figure S1. Soil physiochemical parameters in decomposition soils during the one-year study. Data is shown for each individual donor: SP1 (gold), SP2 (blue), and SP2 (black). Values for the full 16 cm core samples were estimated by summing values interface (0-1 cm) and core (0-16 cm) reported by Taylor et al, (2024) in 1:16 and 15:16 ratios, respectively. Controls reported here are means of three experimental controls that were unimpacted by decomposition and are represented by stars.



Supplementary Material 2: Figure S2. Hierarchical clustering heatmap showing the log counts per million (CPM) of the top 500 most variable genes across samples. Variable genes were determined by selecting genes with the highest variance in gene expression. Samples are clustered along the x-axis using Euclidean distances between samples and colored by study day.

1832

1833

1834

Table S1. Permutational analysis of variance (PERMANOVA) results identifying significant environmental parameters which explain some of the variation in soil gene expression profiles. Environmental parameter data is from Taylor et al. (2024).

1837

1838

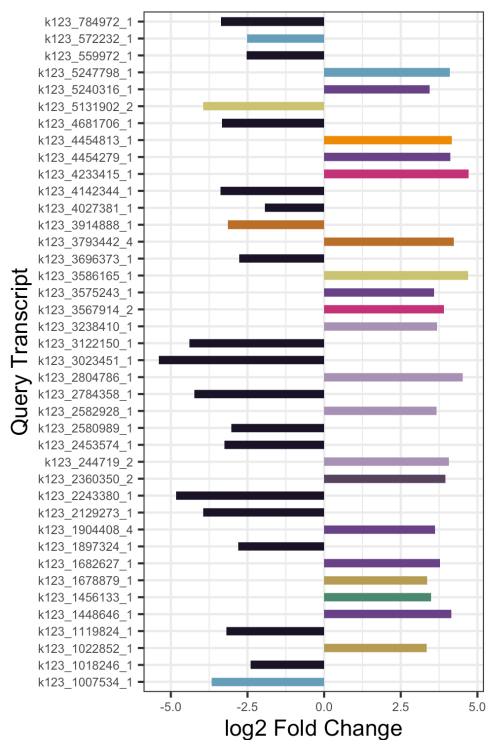
1839

1840

Variables with $p < 0.05$ are indicated in bold.

Supplementary Material 3

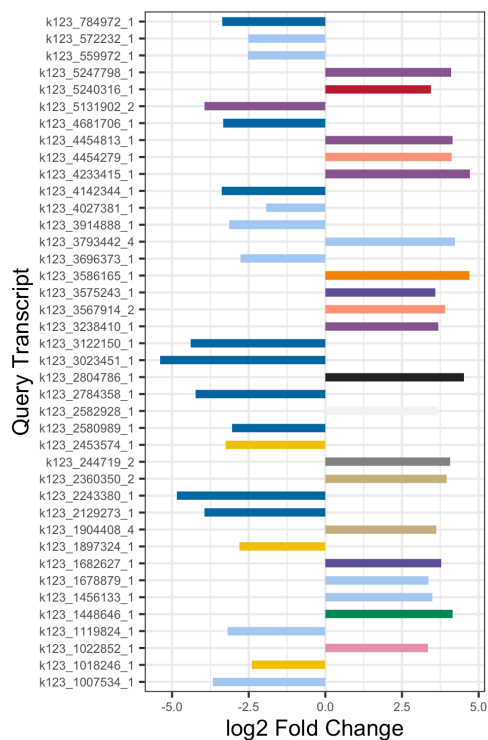
A



COG Category

- Cell motility
- Energy production and conversion
- Transcription
- Cell cycle control, cell division, chromosome partitioning
- Carbohydrate transport and metabolism
- Intracellular trafficking, secretion and vesicular transport
- Signal transduction mechanisms
- Translation, ribosomal structure and biogenesis
- Post-translational modification, protein turnover, and chaperones
- Function Unknown
- unclassified

B



Taxonomy

- 1117|Cyanobacteria
- 1236|Gammaproteobacteria
- 135614|Xanthomonadales
- 2|Bacteria
- 200940|Thermodesulfobacteria
- 201174|Actinobacteria
- 203682|Planctomycetes
- 204432|Acidobacteriia
- 2157|Archaea
- 28211|Alphaproteobacteria
- 28221|Deltaproteobacteria
- 4751|Fungi
- 57723|Acidobacteria
- 976|Bacteroidetes

Supplementary Material 4: Figure S3. Top 30 up- and down-regulated genes in controls relative to decomposition soils across all study days, colored by COG functional category (A) and taxonomic annotation (B). Positive values denote higher expression in controls, while negative values are higher in decomposition soils.

1887
1888
1889
1890
1891
1892
1893
1894 Table S2. Top 15 most up- and down-regulated gene queries, determined by log2 fold
1895 change and adjusted p-values, in control relative to decomposition soils. Positive
1896 log2 fold change values represent genes whose expression was higher in control soils,
1897 while negative log2 fold change values were higher in decomposition soils. Taxonomic
1898 annotation, COG categories, gene description, gene names, and EC were assigned
1899 via eggNOG-mapper.

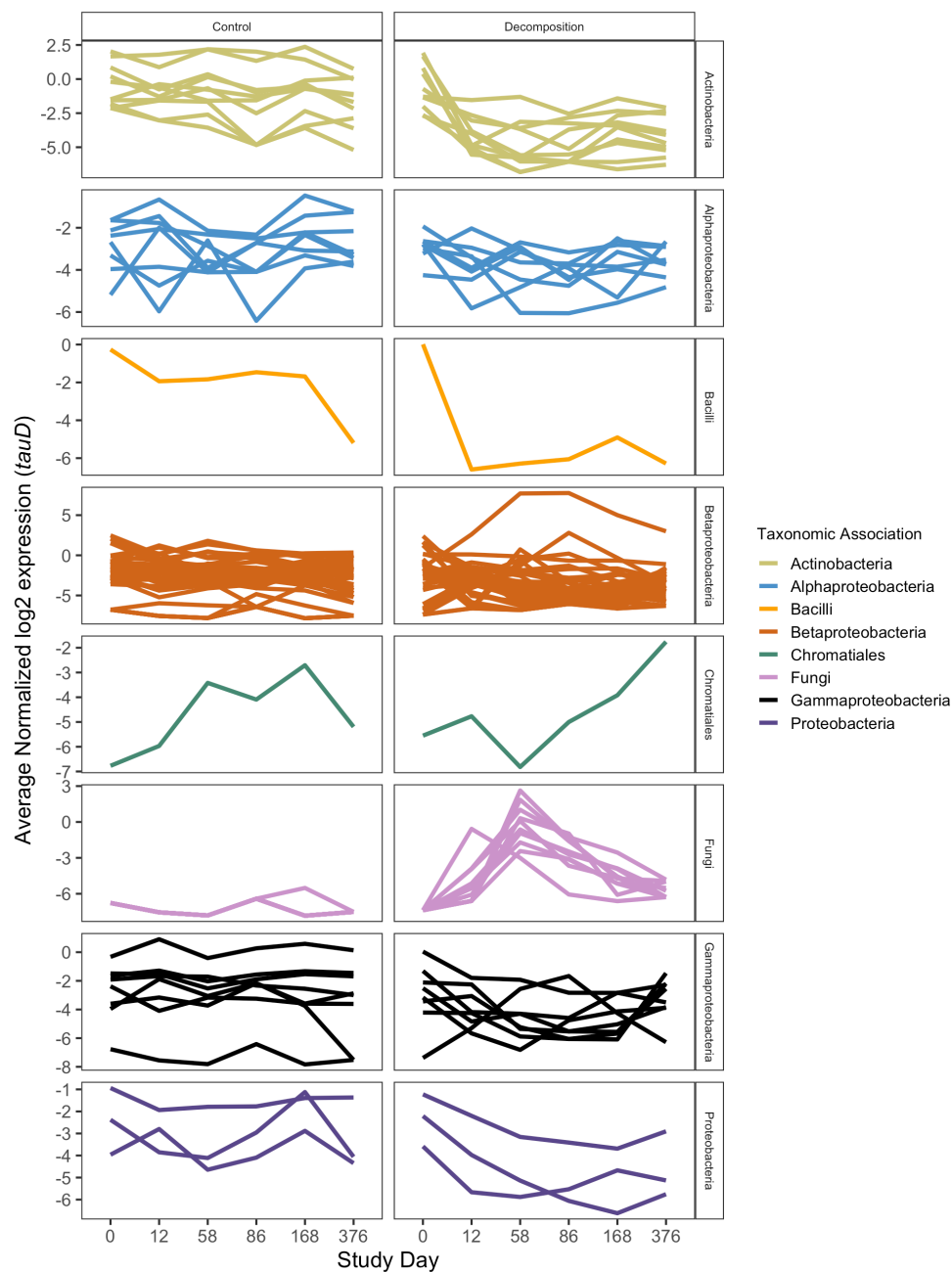
Supplementary Material 5

1900
1901
1902
1903
1904
1905
1906
1907
1908
1909
1910
1911
1912
1913
1914
1915
1916

1917 Table S3. Top 10 most up- and down-regulated genes, determined by log2 fold
1918 change and adjusted p-values, for each sequential timepoint comparison. Positive
1919 log2 fold change values represent genes whose expression was higher in the later
1920 decomposition timepoint soils, while negative log2 fold change values are higher in
1921 earlier decomposition timepoint soils. Taxonomic annotation, COG categories, gene
1922 names, and EC were assigned via eggNOG-mapper. The comparison column
1923 distinguishes each timepoint comparison.

Supplementary Material 6

1924
1925
1926
1927
1928
1929
1930
1931
1932



Supplementary Material 7: Figure S4. Mean normalized log₂ expression of *tauD* genes by taxonomic association (color) in control and decomposition soils at each study day. Each line represents one *tauD* gene query, while color denotes taxonomic association as determined by eggNOG-mapper.